

This article was downloaded by:

On: 24 January 2011

Access details: *Access Details: Free Access*

Publisher *Taylor & Francis*

Informa Ltd Registered in England and Wales Registered Number: 1072954 Registered office: Mortimer House, 37-41 Mortimer Street, London W1T 3JH, UK



## Journal of Macromolecular Science, Part A

Publication details, including instructions for authors and subscription information:

<http://www.informaworld.com/smpp/title~content=t713597274>

### Studies on the Properties of a New Hybrid Materials Containing Hyperbranched Polymer and SiO<sub>2</sub>-TiO<sub>2</sub> Networks

Shao-Rong Lu<sup>ab</sup>; Hailiang Zhang<sup>a</sup>; Caixian Zhao<sup>a</sup>; Xiayu Wang<sup>a</sup>

<sup>a</sup> Institute of Polymer Science and Engineering, Xiangtan University, Xiangtan, Hunan Province, P.R. China <sup>b</sup> Key Laboratory of Nonferrous Metal Materials and New Processing Technology (Institute of Guilin Technology), Ministry of Education, Guilin, Guangxi, P.R. China

**To cite this Article** Lu, Shao-Rong , Zhang, Hailiang , Zhao, Caixian and Wang, Xiayu(2005) 'Studies on the Properties of a New Hybrid Materials Containing Hyperbranched Polymer and SiO<sub>2</sub>-TiO<sub>2</sub> Networks', Journal of Macromolecular Science, Part A, 42: 12, 1691 – 1701

**To link to this Article:** DOI: 10.1080/10601320500247147

**URL:** <http://dx.doi.org/10.1080/10601320500247147>

PLEASE SCROLL DOWN FOR ARTICLE

Full terms and conditions of use: <http://www.informaworld.com/terms-and-conditions-of-access.pdf>

This article may be used for research, teaching and private study purposes. Any substantial or systematic reproduction, re-distribution, re-selling, loan or sub-licensing, systematic supply or distribution in any form to anyone is expressly forbidden.

The publisher does not give any warranty express or implied or make any representation that the contents will be complete or accurate or up to date. The accuracy of any instructions, formulae and drug doses should be independently verified with primary sources. The publisher shall not be liable for any loss, actions, claims, proceedings, demand or costs or damages whatsoever or howsoever caused arising directly or indirectly in connection with or arising out of the use of this material.

# Studies on the Properties of a New Hybrid Materials Containing Hyperbranched Polymer and SiO<sub>2</sub>-TiO<sub>2</sub> Networks

SHAO-RONG LU,<sup>1,2</sup> HAILIANG ZHANG,<sup>1</sup> CAIXIAN ZHAO,<sup>1</sup>  
AND XIAYU WANG<sup>1</sup>

<sup>1</sup>Institute of Polymer Science and Engineering, Xiangtan University, Xiangtan, Hunan Province, P.R. China

<sup>2</sup>Key Laboratory of Nonferrous Metal Materials and New Processing Technology (Institute of Guilin Technology), Ministry of Education, Guilin, Guangxi, P.R. China

*EP/SiO<sub>2</sub>-TiO<sub>2</sub> hybrid materials, which contained hyperbranched polymers (HBPs) chain-extended urea, were prepared through a sol-gel process of triethoxysilyl functionalized HBPs, i.e., chain-extended urea—H<sub>2</sub>O-Si(OC<sub>2</sub>H<sub>5</sub>), Tetraethoxysilane (TEOS) and tetrabutyltitanate (TBT) using HCl as catalyst. The H<sub>2</sub>O-Si(OC<sub>2</sub>H<sub>5</sub>)<sub>3</sub> was obtained by endcapped H<sub>2</sub>O with tolylene 2,4-diisocyanate (TDI), followed by a reaction with 3-aminopropyltriethoxysilane (WD-50). The chemical structure of the products was confirmed by IR spectroscopy. The mechanical properties of composites such as, impact strength, tensile strength, dynamic mechanical thermal properties were investigated. The results showed that the glass transition temperatures and the modulus of the modified systems were higher than that of the unmodified system, and the impact strength was enhanced by two times or that compared with the neat epoxy. The morphological structure of the impact fracture surface and the surface of the hybrid were observed by scanning electron microscope (SEM) and atomic force microscopy (AFM), respectively.*

**Keywords** hybrid materials, epoxy/silica-tinatia, hyperbranched polymers, sol-gel process

## Introduction

Epoxy-based materials have been widely used commercially in modern industries because of low shrinkage on curing, good adhesion to substrate, superior electrical, and mechanical resistance. Frequently, crosslinking is accompanied by embrittlement causing mechanical failure upon straining and impact. It is an important objective to explore new routes toward toughening of epoxy resins without their affecting stiffness, strength, and glass temperature (1).

Received January 2005; Accepted March 2005.

Address correspondence to Xiayu Wang, Institute of Polymer Science and Engineering, Xiangtan University, Xiangtan 411105, Hunan Province, P.R. China. E-mail: wxy36@yahoo.com

Recently, hyperbranched polymers (HBPs) have been widely used for toughening epoxy resin (2–8). Since their Newtonian behavior, low viscosity, and the small dimensions of the hyperbranched polymer, molecules compared to their molecular weight make them extremely suitable as toughness modifiers in low viscosity epoxy resins (2). The specific advantages of the dendritic hyperbranched polymer molecules are that: (a) their chemistry can readily be tailored to have suitable mechanisms; (b) they are reactive; (c) they can readily be made compatible with the surrounding matrix material (9). They are thus particularly applicable to almost any thermoset resin system. Prominent representatives of HBPs used in thermoset toughening are aliphatic polyesters, commercially available from Perstorp polyols under the trade name of Boltorn and various end group modifications are available (10). Manson et al. reported toughening of epoxy resins by epoxy-functional Boltorn. According to these works, the stress intensity factor ( $K_{IC}$ ) values of the prepared resins were improved up to 300%, depending on the degree of modification of the HBP and the curing cycle (8). In contrast, Heiden et al. reported only slightly improved toughness when employing hydroxyl-terminated Boltorn in epoxy formulations (11). The improvement of fracture toughness by the addition of HBP modifiers, however, is frequently associated with softening of the matrix due to matrix flexibilization. This is not unexpected since the modulus and glass transition temperature of the modifiers is much lower than that of the matrix (12).

Nanocomposites technology using metal alkoxide as *in situ* route to nanoreinforcement offers new opportunities for the modification of thermoset micromechanics. Large improvements of mechanical and physical properties including modulus (13), barrier properties (14) and flammability resistance (15) have been reported for this type of material at low inorganic nanoparticles. In principle, it should be possible to compensate matrix flexibilization via matrix reinforcement using inorganic nanoparticles.

This paper presents results of a new strategy to produce toughened epoxy resins with a high modulus and glass transition temperature. A ternary cured networks with epoxy resin, hydroxyl functionalized hyperbranched polymer and  $\text{SiO}_2\text{-TiO}_2$  formed by a sol-gel process, has been obtained in this composite. In this work, HBP was used as the toughening agent and the inorganic  $\text{SiO}_2\text{-TiO}_2$  nanoparticles may help recover some of the rigidity lost due to the addition of toughening agents, and may also contribute to improve toughness as well. Dynamic mechanical analysis (DMA), mechanical testing, X-ray diffraction (XRD), and scanning electron microscopy (SEM) were used to examine the thermal, mechanical and morphological behaviors of the hybrid materials.

## Experimental

### Materials and Measurements

Boltorn<sup>TM</sup> 20 (H20) was provided by Perstorp AB Company (Sweden) and used directly. The epoxy resin need (diglycidyl ether of bisphenol A, DGEBA(E-51),  $\text{Wep} = 196$ ) was purchased from Yueyang Chemical Plant (China) without further purification). 3-aminopropyltrimethoxysilane (WD-50) was purchased from Chemical Reagent Co. of Wuhan University (China) and was purified by distillation before use. Toluenediisocyanate (TDI) (80/20) was purified by distillation under vacuum, 4,4'-diaminodiphenylsulphone (DDS) was obtained from Shanghai Chemical Reagent Company (China) with a molecular mass of 248.31 and purity >96% according to the supplier. Tetraethoxysilane (TEOS) and Tetrabutyltitanate (TBT) (both chemical reagent grade) were ordered from Xilong Chemical Factory, Guangdong (China). Fourier transformed infrared spectroscopy

(FT-IR) was recorded between 4000 and 400  $\text{cm}^{-1}$  on a Perkin-Elmer 1710 instrument using KBr pellets for organic polymer samples. The crystalline behavior of the EP and EP/SiO<sub>2</sub>-TiO<sub>2</sub> material were analyzed by X-ray diffractometry (XRD: D/max-RB, Japan). UV-Vis spectra were measured on a Shimadzu UV-265 Spectrophotometer. The impact strength was measured on a tester, XJJ-5, with no notch in the specimen. According to the China National Standard GB1043-79, the size of the sample was  $4.0 \times 10.0 \times 80 \text{ mm}^3$ . The tensile strength was examined on an electron omnipotence tester of type RGT-5, at the rate of  $2 \text{ mm} \cdot \text{min}^{-1}$ . According to the China National Standard GB1040-92, all the presented results are the average of five specimen tests. Dynamic mechanical analysis (DMA) was made with a TA Instruments (902-50010 dynamic mechanical analyzer) under a frequency of 1 Hz from  $-120^\circ\text{C}$  to  $25^\circ\text{C}$  at a heating rate of  $5^\circ\text{C}/\text{min}$ . The rectangular bending mode was chosen and the dimensions of the specimen were  $48 \times 5 \times 2.5 \text{ mm}^3$ . Atomic force microscopy (AFM) was carried out using AJ-IIIa (Shanghai AJ Nano-Science Development Co. Ltd). The scan rate is 2.00061 Hz, scan size 5.00061, number of sample 256.

#### **Preparation of Sol-Gel Precursor H2O-Si(OC<sub>2</sub>H<sub>5</sub>)<sub>3</sub>**

5.36 g (3.07 mmol) H2O dissolved in the proper amount of acetone was added into a three-necked round-bottomed flask equipped with a mechanical stirrer, a N<sub>2</sub> inlet-outlet and a cooler. The mixture of 7.0 mL TDI and 10 mL acetone was then dropped into the flask within 1 h. The solution was stirred for an additional 20 h at  $30^\circ\text{C}$ , and a yellow solution was obtained. The terminal of the reaction was confirmed by titration of the isocyanate group content. A certain amount of WD-50 and acetone mixture were then dropped into the above solution within 3 h and stirred at  $30^\circ\text{C}$  for additional 1 day. The acetone was distilled under vacuum at  $50^\circ\text{C}$  to get the final precursor H2O-Si(OC<sub>2</sub>H<sub>5</sub>)<sub>3</sub>.

#### **Preparation of Sol-Gel Precursor for Hybrid Materials**

In a 250 mL round-bottom flask, about 100 g epoxy resin, an appropriate amount of H2O-Si(OC<sub>2</sub>H<sub>5</sub>)<sub>3</sub>, TBT, TEOS, hydrochloric acid, distilled H<sub>2</sub>O and Tetrahydrofuran (THF) were introduced. After vigorous stirring for 30 min, the mixture became homogenous. Then, the solution was transferred into a 250 mL beaker covered with parafilm to allow the evaporation of small molecules for a few days. The epoxy/silica-titania hybrid precursors were obtained. The contents of all the components in various samples are shown in Table 1.

#### **Curing Procedure**

A mixture of epoxy/silica-titania hybrid precursor and a stoichiometric amount of DDS (30 g per 100 g of epoxy resin) was degassed in vacuum at  $130^\circ\text{C}$  for about 30 min. The resulting mixture was then cast into a preheated mold coated with silicone resin. All samples were cured at  $120^\circ\text{C}$  for 2 h,  $150^\circ\text{C}$  for 2 h, and  $170^\circ\text{C}$  for 2 h.

## **Results and Discussion**

#### **Characterization of the Hybrid Materials**

As mentioned in section 2, the preparation of the hybrid materials included three steps. The possible reactions are shown in Scheme 1. Step1 was a hydrogen shift reaction

**Table 1**  
Sample preparation and composition<sup>a</sup>

| Sample | EP<br>(g) | TBT<br>(g) | TEOS<br>(g) | H2O-Si(OC <sub>2</sub> H <sub>5</sub> ) <sub>3</sub><br>(g) | SiO <sub>2</sub> -TiO <sub>2</sub> <sup>b</sup><br>(wt%) | Impact strength<br>(KJ/m <sup>2</sup> ) |
|--------|-----------|------------|-------------|---|--|---|
| 0      | 100       | 0          | 0           | 0   | 0  | 11.6                                    |
| 1      | 100       | 0.75       | 1.8         | 10  | 1.67   | 24.8                                    |
| 2      | 100       | 1.50       | 3.6         | 10  | 2.23   | 26.7                                    |
| 3      | 100       | 2.25       | 5.4         | 10  | 2.78   | 27.5                                    |
| 4      | 100       | 2.95       | 7.2         | 10  | 3.30   | 23.6                                    |
| 5      | 100       | 1.50       | 3.6         | 5   | 1.81   | 18.7                                    |
| 6      | 100       | 1.50       | 3.6         | 15  | 2.65   | 27.8                                    |
| 7      | 100       | 1.50       | 3.6         | 0   | 3.00   | 24.3                                    |

<sup>a</sup>Preparation condition: [H<sub>2</sub>O]: [TEOS + TBT] = 1 : 1, [HCl]: [TEOS + TBT] = 0.05 (mol. rate).

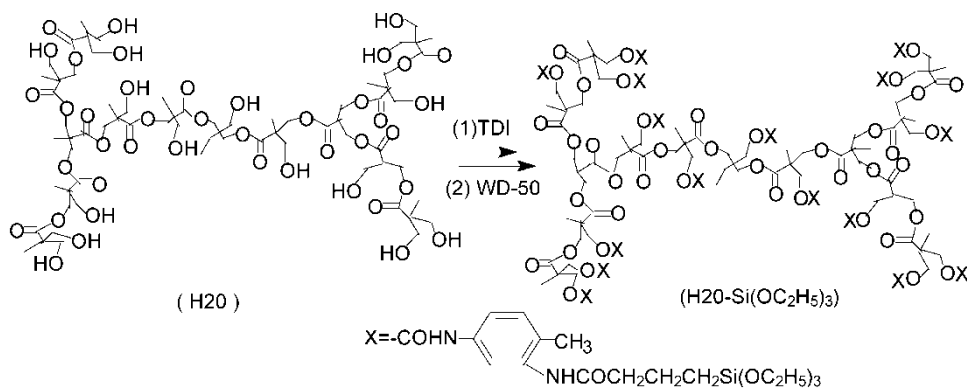
<sup>b</sup>Silica and titania contents were calculated theoretically.

between tolylene 2,4-diisocyanate (TDI) and H2O, resulting in producing the endcapped H2O. Since the molar ratio of TDI/H<sub>2</sub>O was 16/1, basically only one of the -NCO groups on TDI could participate in this reaction and all of the -OH groups on H2O was endcapped. Step 2 is a coupling reaction of WD-50 with the endcapped H2O. In this step, the -NH<sub>2</sub> groups of WD-50 reacted with the -NCO groups of the endcapped H2O, forming carbamido linkage—H2O-Si(OC<sub>2</sub>H<sub>5</sub>)<sub>3</sub>, which contains -Si(OC<sub>2</sub>H<sub>5</sub>)<sub>3</sub> and -NH groups. Step 3 is the preparation of EP/SiO<sub>2</sub>-TiO<sub>2</sub> hybrid materials. This step includes two steps, first, epoxy, H2O-Si(OC<sub>2</sub>H<sub>5</sub>)<sub>3</sub>, Si(OC<sub>2</sub>H<sub>5</sub>)<sub>4</sub> and Ti(OC<sub>4</sub>H<sub>9</sub>)<sub>4</sub> were hydrolyzed by using hydrochloric acid as the catalyst and THF as the solvent, and produced the precursors of the hybrid materials. The other step is a curing reaction of the precursor of hybrid materials with DDS as curing agent forming polymer network.

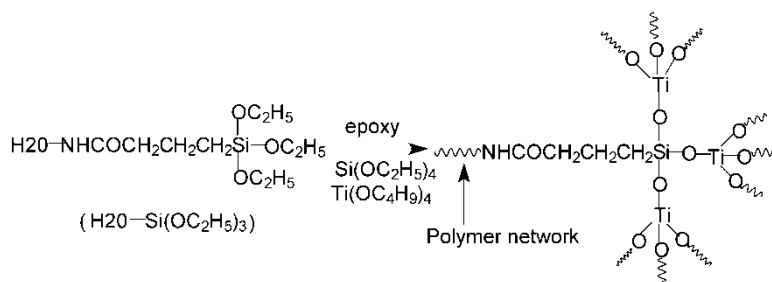
Figure 1 shows the FT-IR spectra of (a) H2O (b) endcapped H2O (c) H2O-Si(OC<sub>2</sub>H<sub>5</sub>)<sub>3</sub> (d) EP/SiO<sub>2</sub>-TiO<sub>2</sub> hybrid material. In (a), a distinct absorption peak at ~1100 cm<sup>-1</sup> is in the region of -C-O-C stretching for ether groups and the peak at 3474 cm<sup>-1</sup> belongs to -OH group. In (b) the peak at ~2274 cm<sup>-1</sup> confirms the existence of -NCO groups. In (c) the disappearance of isocyanate peak at 2274 cm<sup>-1</sup> and formation N-H peak of urethane group at 3327 cm<sup>-1</sup> and 1590–1520 cm<sup>-1</sup>, while the peak at ~1100 cm<sup>-1</sup> increased and broadened since the -C-O-C stretching overlapped with Si-O-C stretching band. In (d) the peak at 3413 cm<sup>-1</sup>, (characteristic of -OH stretching, which is the unreactive Ti-OH or Si-OH groups in inorganic networks) and 1108 cm<sup>-1</sup> (characteristic of Si-O-C). In addition, there was also the broad absorption at lower wavenumber region. Especially 1100~920 cm<sup>-1</sup> (characteristic of Si-O-Si and Si-O-Ti networks) at 900~450 cm<sup>-1</sup> due to Ti-O-Ti linkage in the titania matrix. The band at around 950 cm<sup>-1</sup> is attributed to Si-O-Ti bonds (16).

### Mechanical Performance

The impact resistance property of the cured epoxy with different contents of H2O-Si(OC<sub>2</sub>H<sub>5</sub>)<sub>3</sub> and SiO<sub>2</sub>-TiO<sub>2</sub> nanoparticles were evaluated on a Charpy impact testing machine, and the results are listed in Table 1. It is very clear that the addition of the H2O-Si(OC<sub>2</sub>H<sub>5</sub>)<sub>3</sub>, TBT and TEOS significantly improves the toughness of the cured



Step 1. Coupling WD-50 endcapped H2O



Step 2. The preparation of EP/SiO<sub>2</sub>-TiO<sub>2</sub> hybrid materials

**Scheme 1.** The step reactions for preparing EP/SiO<sub>2</sub>-TiO<sub>2</sub> hybrid materials.

epoxy resin. In this study, H2O-Si(OC<sub>2</sub>H<sub>5</sub>)<sub>3</sub> and SiO<sub>2</sub>-TiO<sub>2</sub> nanoparticles act as a softer second phase and a stress concentrators, respectively.

Table 1 also shows the impact toughness of the composites increases slightly with SiO<sub>2</sub>-TiO<sub>2</sub> contents. Since unnotched Charpy impact strength reflects the energy consumed before fracture, and SiO<sub>2</sub>-TiO<sub>2</sub> nanoparticles in the composites are able to induce plastic deformation of the surrounding matrix polymer to a certain extent under

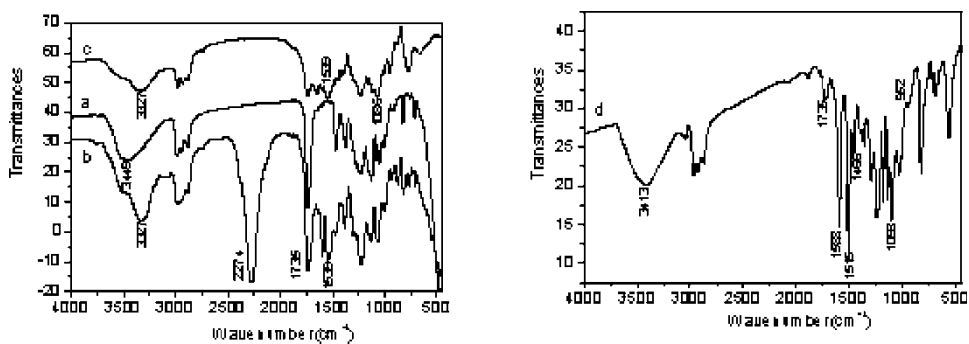


**Figure 1.** The FT-IR absorption peaks of (a) H2O, (b) endcapped H2O, (c) H2O-Si(OC<sub>2</sub>H<sub>5</sub>)<sub>3</sub>, and (d) EP/SiO<sub>2</sub>-TiO<sub>2</sub> hybrid material.

the high strain rate conditions. The results of Table 1 show that the impact strength reaches the highest level for  $\text{SiO}_2\text{-TiO}_2$  contents about 2.78 wt% or so. The impact strength decreases gradually with  $\text{SiO}_2\text{-TiO}_2$  contents increasing. Although  $\text{SiO}_2\text{-TiO}_2$ /epoxy matrix adhesion is improved, agglomeration of the  $\text{SiO}_2\text{-TiO}_2$  nanoparticles is severe in the high  $\text{SiO}_2\text{-TiO}_2$  content ( $>3.0$  wt%). However, it remains well above the performance of the pure epoxy.

Figure 2 shows the relation between  $\text{H}_2\text{O-Si}(\text{OC}_2\text{H}_5)_3$  content and tensile strength and modulus. The experiment results indicated that both tensile strength and modulus increase with  $\text{H}_2\text{O-Si}(\text{OC}_2\text{H}_5)_3$  content increasing. The addition of  $\text{H}_2\text{O-Si}(\text{OC}_2\text{H}_5)_3$  beneficially improved the tensile strength of the modified system, it reached a maximum (78 Mpa) when the  $\text{H}_2\text{O-Si}(\text{OC}_2\text{H}_5)_3$  content was up to 15 wt%. This value was 47% higher than that of the unmodified system (53 Mpa). The tensile strength decreased while the  $\text{H}_2\text{O-Si}(\text{OC}_2\text{H}_5)_3$  content was more than 15 wt%, but it was still 30% higher than that of the unmodified system. The modulus of the modified system had the same behavior as the tensile strength, and it was 14.8% higher than the unmodified system when the  $\text{H}_2\text{O-Si}(\text{OC}_2\text{H}_5)_3$  content was 15 wt%. The tensile modulus increased at first and then decreased with the increase of the  $\text{H}_2\text{O-Si}(\text{OC}_2\text{H}_5)_3$  content.

### XRD Analysis

Figure 3 shows the XRD patterns of the EP and EP/ $\text{SiO}_2\text{-TiO}_2$  hybrid materials. It can be seen that the patterns of EP and EP/ $\text{SiO}_2\text{-TiO}_2$  are very similar. Both of them have a broad amorphous peak. The contact angle of the peaks is between  $5^\circ$  and  $30^\circ$ . It means that  $\text{SiO}_2\text{-TiO}_2$  networks and epoxy matrix incorporated through the covalent and hydrogen bond, and did not simple mixing. This is also proved by the FT-IR spectrum.

### Morphology of the Fractured Surface

The impact fracture surfaces of the hybrid samples were observed by SEM. Some representative specimens were chosen to study the deformation mechanism. Figure 4 shows the morphology of the impact fracture surface of the hybrid materials with different  $\text{SiO}_2\text{-TiO}_2$  contents. It can be seen that the morphologies of the epoxy resins modified with

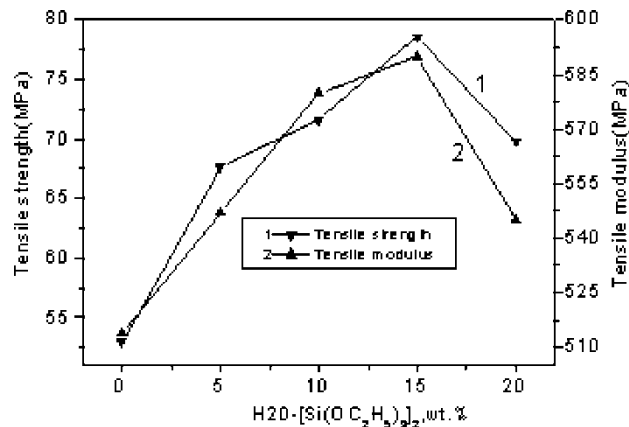


**Figure 2.** The relation between  $\text{H}_2\text{O-Si}(\text{OC}_2\text{H}_5)_3$ , wt% and tensile strengths and tensile modulus.

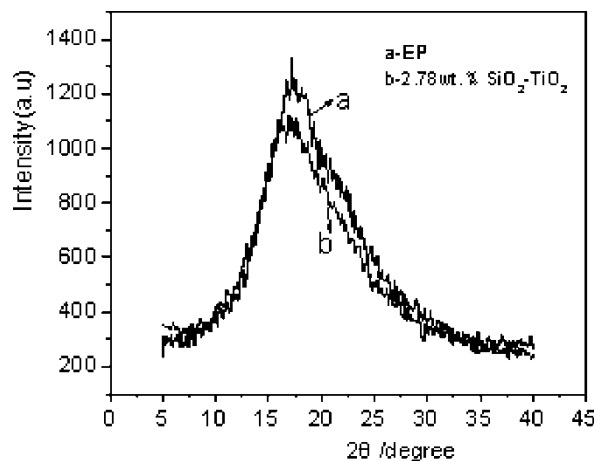


**Figure 3.** X-ray diffraction patterns of the EP and EP/SiO<sub>2</sub>-TiO<sub>2</sub> hybrid material.

H<sub>2</sub>O-Si(OC<sub>2</sub>H<sub>5</sub>)<sub>3</sub> are quite different from that of the unmodified system. The fracture surface of the unmodified system reveals a brittle behavior characterized by large smooth veining and fracture steps in the direction of crack propagation, which indicates a weak resistance to crack propagation. As for the modified systems, the fracture surfaces present a rough and irregular appearance with many holes or indentations, which indicates that there are many micro-phase-separation uniform distribution in the

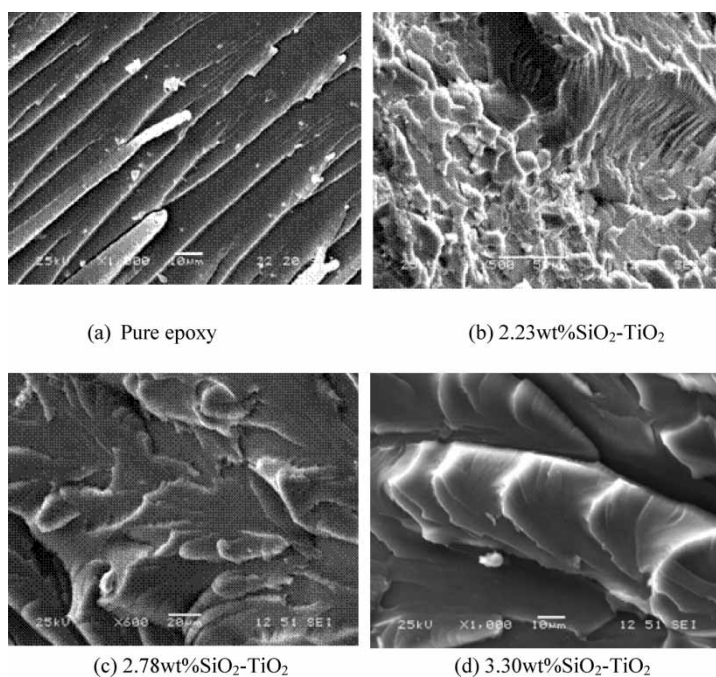


**Figure 4.** SEM graphs of hybrid materials with the different SiO<sub>2</sub>-TiO<sub>2</sub> contents.



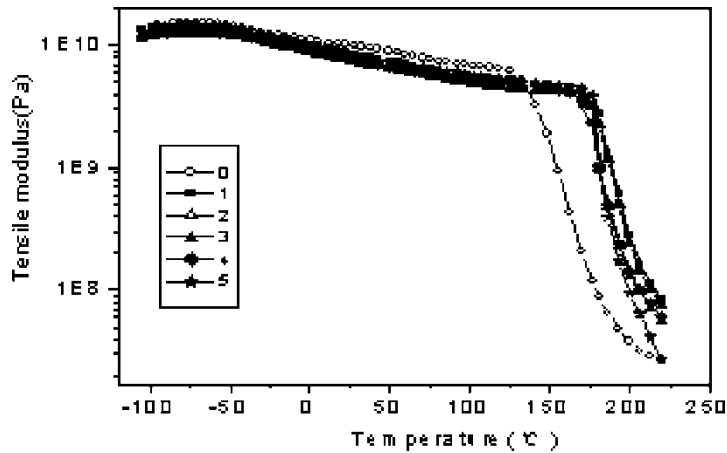


Figure 5. Modulus vs. temperature for curing system.

fracture surface. It can consume a large amount of energy under impact process and disperse stress, indicating the characteristic of toughening fracture. This is in very good agreement with the impact resistance property of the hybrid materials shown in Table 1.

#### Dynamic Mechanical Behavior

The storage modulus data of the modified system and unmodified system are shown in Figure 5. It can be seen that below 110°C the storage modulus of the modified systems is approximate to that of the pure EP. As we know, when rubbery components are used to modify epoxy resin, the modulus is usually sacrificed at elevated temperature. Similar observation was reported by D. Ratna et al. (17) for HBPs and epoxy resin systems. However, the modified system prepared in this work consisted of HBPs frame with SiO<sub>2</sub>-TiO<sub>2</sub> inorganic particle in the network. It must be the rigid SiO<sub>2</sub>-TiO<sub>2</sub> inorganic networks play a great role in maintaining the high modulus of the cured hybrid materials. With the temperature increasing, the modulus of the modified system (4.3E9) appears much higher than that of the unmodified system (1.8E8) at 170°C,

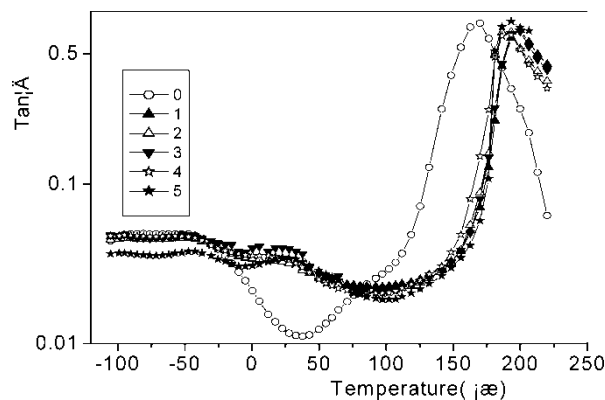


Figure 6. Mechanical loss vs. temperature for curing system.

**Table 2**The loss tangent values ( $\tan \delta$ ) and glass transition temperatures of the cured system

| No. | H2O-Si(OC <sub>2</sub> H <sub>5</sub> ) <sub>3</sub> wt% | $\tan \delta$ | T <sub><math>\beta</math></sub> (°C) | T <sub><math>\alpha</math></sub> (°C) |
|-----|--|---------------|--------------------------------------|---------------------------------------|
| 0   | 0  | 0.712         | -57.284                              | 169.8                                 |
| 1   | 5 (SiO <sub>2</sub> -TiO <sub>2</sub> 1.81 wt%)          | 0.653         | -46.807                              | 189.8                                 |
| 2   | 10 (SiO <sub>2</sub> -TiO <sub>2</sub> 2.23 wt%)         | 0.639         | -47.543                              | 192.0                                 |
| 3   | 15 (SiO <sub>2</sub> -TiO <sub>2</sub> 2.65 wt%)         | 0.644         | -47.19                               | 192.2                                 |
| 4   | 20 (SiO <sub>2</sub> -TiO <sub>2</sub> 3.00 wt%)         | 0.621         | -55.01                               | 189.6                                 |
| 5   | 10 (SiO <sub>2</sub> -TiO <sub>2</sub> 1.67 wt%)         | 0.682         | -41.57                               | 190.6                                 |

indicating that the motion of the molecular chains in the materials is strongly restricted by the HBPs network and SiO<sub>2</sub>-TiO<sub>2</sub> inorganic network. These phenomena were also observed in other hybrids materials (18, 19).

The loss tangent data of the hybrid materials are shown in Figure 6. The peak values and temperature of the transition are summarized in Table 2. It can be seen that all the specimen exhibit  $\alpha$ - and  $\beta$ -relaxation peak. The peak values of  $\tan \delta$  for modified system appear to be slightly decreased with H2O-Si(OC<sub>2</sub>H<sub>5</sub>)<sub>3</sub> content increasing. The  $\tan \delta$  peak temperature for the modified systems are considerably higher than that of the unmodified system, indicating that the addition of H2O-Si(OC<sub>2</sub>H<sub>5</sub>)<sub>3</sub>, TEOS and TBT in materials made it difficult for the chain segments moving, therefore, the glass transition temperatures (T<sub>g</sub>) of the hybrid materials were shifted to a higher temperature. It is possibly attributed by the co-effect of the HBPs network and the SiO<sub>2</sub>-TiO<sub>2</sub> inorganic network.

#### AFM Surface Image of Hybrid Material

The surface topography structure of the hybrid film (2.78% SiO<sub>2</sub>-TiO<sub>2</sub> content) is characterized by AFM (Figure 7). The film thickness is about 20 nm, the scan area is

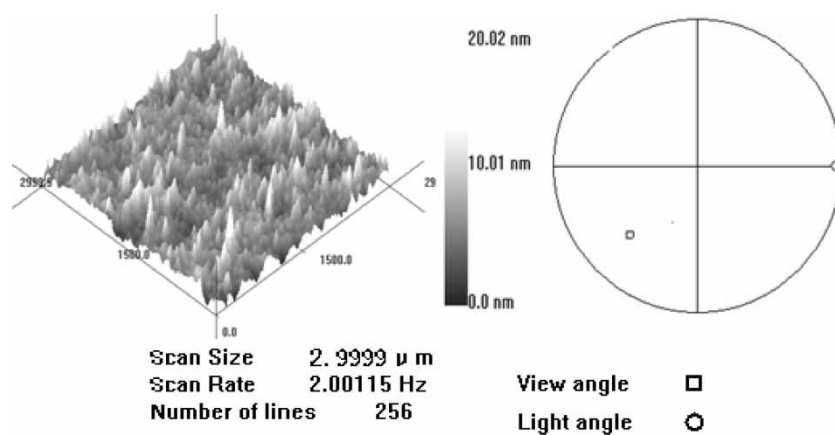


**Figure 7.** AFM surface images of the SiO<sub>2</sub>-TiO<sub>2</sub> composite specimen. The scan area is 3  $\mu$ m  $\times$  3  $\mu$ m.

3  $\mu\text{m} \times 3 \mu\text{m}$ . From the micrograph, it can be seen that the  $\text{SiO}_2\text{-TiO}_2$  particle size is about 20–60 nm, and the  $\text{SiO}_2\text{-TiO}_2$  particles are homogeneously dispersed in the hybrid material matrix.

## Conclusions

A new hybrid material incorporating  $\text{H}_2\text{O-Si(OC}_2\text{H}_5)_3$  with inorganic compounds ( $\text{Ti(OC}_4\text{H}_9)_4$  and  $\text{Si(OC}_2\text{H}_5)_4$ ) via sol-gel process has been successfully prepared. The experimental results showed the silica and titania particle size in the hybrid films was about 20–60 nm. The impact strength of the cured systems modified with  $\text{H}_2\text{O-Si(OC}_2\text{H}_5)_3$  was 2 times higher than that of the unmodified epoxy. The glass transition temperatures ( $T_g$ ) of the hybrid materials are much higher than that of the unmodified system, and the fracture surfaces of all modified systems exhibit the character of tough fracture feature.

## Acknowledgements

Financial support from the Natural Science Foundation of GuangXi Province (No. 0447053) is gratefully acknowledged.

## References

1. Kinloch, A.J. and Shaw, H. (1983) Deformation and Fracture Behavior of Rubber-Toughened Epoxy: 1. Microstructure and Fracture Studies. *Polymer*, 24 (10): 1341–1352.
2. Boogh, L., Pettersson, B., and Manson, J.A.E. (1999) Dendritic Hyperbranched Polymers as Tougheners for Epoxy Resins. *Polymer*, 40 (9): 2249–2261.
3. Sidorenko, A., Zhai, X.W., Simon, F., Pleul, D., and Tsukruk, V.V. (2002) Hyperbranched Molecules with Epoxy-Functionalized Terminal Branches: Grafting to a Solid Surface. *Macromolecules*, 35 (13): 5131–5139.
4. Ratna, D. and Simon, G. (2001) Thermomechanical Properties and Morphology of Blends of a Hydroxy-Functionalized Hyperbranched Polymer and Epoxy Resin. *Polymer*, 42 (21): 8833–8839.
5. Joon, H.O., Jongsik, J., and Suck-Hyun, L. (2001) Curing behavior of Tetrafunctional Epoxy resin/hyperbranched Polymer System. *Polymer*, 42 (20): 8339–8347.
6. Mezzenga, R., Plummer, C.J.G., Boogh, L., and Manson, J.-A.E. (2001) Morphology Build-Up in Dendritic Hyperbranched Polymer Modified Epoxy Resins: Modeling and Characterization. *Polymer*, 42 (1): 305–317.
7. Emrick, T., Chang, H.-T., and Frechet, J.M.J. (1999) An  $A_2 + B_3$  Approach to Hyperbranched Aliphatic Polymers Containing Chain End Epoxy Substituents. *Macromolecules*, 32 (19): 6380–6382.
8. Boogh, L., Pettersson, B., Anders, J., and Manson, E. (1999) Dendritic Hyperbranched Polymers as Tougheners for Epoxy Resins. *Polymer*, 40 (9): 2249–2261.
9. Shi, W.F. and Ranby, B. (1996) Photopolymerization of Dendritic Methacrylated Polyesters. I. Synthesis and Properties. *J. Appl. Polym. Sci.*, 59 (12): 1937–1944.
10. Fröhlich, J., Kautz, H., Thomann, R., Frey, H., and Müllhaupt, R. (2004) Reactive Core/Shell Type Hyperbranched Blockcopolyethers as New Liquid Rubbers for Epoxy Toughening. *Polymer*, 45 (7): 2155–2164.
11. Wu, H., Xu, J., Liu, Y., and Heiden, P. (1999) Investigation of Readily Processable Thermoplastic-Toughened Thermosets. V. Epoxy Resin Toughened with Hyperbranched Polyester. *J. Appl. Polym. Sci.*, 72 (2): 151–163.

12. Ratna, D., Becker, O., and Krishnamurthy, R. (2003) Nanocomposites Based on a Combination of Epoxy Resin, Hyperbranched Epoxy and a Layered Silicate. *Polymer*, 44 (24): 7449–7457.
13. Wang, M.S. and Pinnavaia, T.J. (1994) Clay-Polymer Nanocomposites Formed From Acidic Derivatives Of Montmorillonite and Epoxy Resin. *Chem. Mater.*, 6): 468–474.
14. Flipsen, T.A.C., Derks, R., Vander Vegt, H.A., Pennings, A.J., and Hadziio-Annou, G. (1997) Densely Cosslinked Polycarbosiloxanes. I. Synthesis. *J. Polym. Sci., Part A: Polym. Chem.*, 35 (1): 41–53.
15. Gilman, J.W., Kashiwagi, T., and Lichtenhan, J.D. (1997) Nanocomposites: A Revolutionary New Flame Retardant Approach. *SAMPE J.*, 33 (4): 40–46.
16. Inorganics IR Grating Spectra. Sadlter Research Laboratories: Philadelphia, Sadlter, 1965; Vols. 1–2, Y249k.
17. Ratna, D. and Simon, G.P. (2001) Thermo-mechanical Properties and Morphology of Dends of a Hydroxy-Functionalized Hyperbranched Polymer and Epoxy Resin. *Polymer*, 42 (21): 8833–8839.
18. Hu, Q. and Marand, E. (1999) *In situ* Formation of Nanosized TiO<sub>2</sub> Domains Within Poly(amide-imide) by a Sol-Gel Process. *Polymer*, 40 (17): 4833–4843.
19. Ahmad, Z., Sarwar, M.I., Wang, S., and Mark, J.E. (1997) Preparation and Properties of Hybrid Organic-Inorganic Composites Prepared From Poly(phenylene)terephthalamide and Titania. *Polymer*, 38 (17): 4523–4529.